Online ISSN: 2981-0396 Print ISSN: 2981-0388

International Journal of Iron & Steel Society of Iran

Journal Homepage: https://journal.issiran.com/

Research Article

Effect of Heat Treatment on The Microstructure and High-Temperature Mechanical Properties of Waspaloy Superalloy

M. Morakabati *[1], M. Oraki [2], M. seifollahi [3], A. Akhondzadeh [4]

Faculty of Materials & Manufacturing Technologies, Malek Ashtar University of Technology, Tehran, Iran

ARTICLE INFO

Keywords:

Waspaloy superalloy, Cold rolled, Hot rolled, Aging, Hot tensile, Stress rupture.

Article history:

Received 30 November 2024
Received in revised form 08 March 2025
Accepted 04 August 2025

ABSTRACT

Waspaloy is a wrought Ni-based superalloy that is widely used in high-temperature structural applications requiring strength retention and performance at elevated temperatures, such as gas turbine engines and aerospace components. This study primarily focuses on the exploration of the impact of heat treatment on the microstructure and high-temperature mechanical properties of the Waspaloy superalloy. The experiment involved processing the alloy in both hot-rolled and cold-rolled conditions, followed by stabilization at 845 °C and aging at various temperatures: 730 °C, 760 °C and 800 °C. Subsequent mechanical property evaluations were conducted using hardness, hot tensile, and stress rupture tests. To examine the microstructural changes, we employed optical and scanning electron microscopy. Our findings revealed that the cold-rolled specimen, aged at 730 °C, exhibited the highest hardness, 581 Vickers. Moreover, our hot tensile test results showed a maximum yield strength of 1340 MPa and an ultimate tensile strength of 1404 MPa for the cold-rolled specimen after aging at 730 °C. The stress rupture test revealed a rupture time of 46 hours for the cold-rolled specimens and 36 hours for the hot-rolled specimens, attributable to the increased size and volume fraction of γ' precipitates in the cold-rolled alloy.

1. Introduction

The Waspaloy superalloy, a nickel-based superalloy characterized by its precipitation-hardening properties, stands as a key component in high-temperature applications. This superalloy's remarkable attributes include maintaining mechanical integrity above 750 °C and demonstrating high-temperature corrosion and oxidation resistance. Waspaloy is a popular choice in industries that operate in extreme temperatures, such as spacecraft and rocket systems, as well as parts of aircraft turbine engines, including discs and blades [1-2].

Given the high working temperatures of components such as discs and vanes, the Waspaloy superalloy is an ideal choice due to its stabilization of mechanical properties—such as creep strength—at elevated temperatures. Its microstructure comprises γ' phases and carbide precipitate primarily in the form of MC, M_6C, and $M_{23}C_6$ [1-4]. The morphology and distribution of these carbides significantly influence the mechanical behavior of the superalloy. For instance, carbides finely dispersed along the grain boundaries can enhance strength, reduce

* *Corresponding Author*
Email: m_morakabati@mut.ac.ir
Address: Faculty of Materials & Manufacturing Technologies, Malek Ashtar University of Technology, Tehran, Iran
1. Associate Professor, 2. Ph.D. Candidate, 3. Associate Professor, 4. M.S.

DOI: http://10.22034/IJISSI.2025.2046934.1312
Published by ISSI (Iron & Steel Society of Iran)

grain boundary sliding, and improve creep and rupture strength [2-3]. The heat treatment of Waspaloy typically involves three stages: solution annealing, stabilization, and final aging. The primary objective of the aging process is to encourage a balanced distribution of γ' precipitates within the matrix. Cold deformation before heat treatment can significantly influence the mechanical properties of Waspaloy, making it crucial to control factors such as cold work reduction and the time and temperature of heat treatment [5-6]. The mechanical properties of the alloy, such as hardness, creep strength, and overall strength, depend largely on factors like grain size and the size and distribution of the varying phases. Therefore, it is imperative to assess the hardness and high-temperature strength of the alloy for design and inspection purposes. Accurate determination of the hardness and strength of high-temperature materials is crucial for maintaining safety standards, making informed economic decisions, and ensuring the timely replacement of parts with low remaining life. Existing research suggests that the aging time and temperature can significantly alter the microstructure of superalloys [7-9]. Despite the significance of heat treatment variables on the microstructure and mechanical properties of the Waspaloy superalloy, research in this area remains somewhat limited [9]. For instance, one study examined the influence of grain size and hardness of 25 mm-thick Waspaloy on cemented carbide tools. The deposition method has been mentioned in the research. The findings revealed that a decrease in grain size from 138 to 45 μm led to an increase in the alloy's hardness from 360 to 390 Vickers. In another study, researchers [9] investigated the effect of aging heat treatment at varying temperatures and durations on the microstructure of 13 mm thick Waspaloy. This research showed that the size of γ' precipitates rose from 10 to 60 nm as the aging temperature increased from 725 to 875 ℃ over a period of 100 hours. The paramount challenge of the Waspaloy superalloy lies in the reduction of its strength and hardness during operation, which in turn decreases the lifespan of parts fabricated from this material. Therefore, preserving the alloy's strength and understanding the mechanisms that underpin its strengthening are key areas of focus in ongoing research. This reduction in strength is primarily a consequence of microstructural alterations that occur during creep [4, 10]. No research has been conducted on the effect of thermomechanical history, including hot-worked and cold-worked conditions, on the Waspaloy alloy with thicknesses of 1 mm and 3 mm, on its response to heat treatment and subsequent high-temperature mechanical properties. Consequently, research has frequently focused on the relationship between the microstructure changes and the mechanical properties of superalloys, a critical approach to determining the optimal aging temperature and duration for specimens. This study aims to investigate the impact of aging heat treatment on the microstructure, hardness and high-temperature mechanical properties of Waspaloy superalloy following both hot and cold working. Modifying the temperature and aging time of the alloy can affect key factors like grain size, volume fraction, and the size of γ' precipitates, which in turn can influence the material's strength behavior. Therefore, through hardness tests and evaluation of high-temperature mechanical properties, we will conduct a meticulous study of the microstructure evolution. The objective is to gain insights into the relationship between the microstructure, hot tensile properties and stress rupture of the alloy.

2. Materials and Methods

The Waspaloy superalloy underwent a melting and alloying process using the vacuum induction melting (VIM) and electro-slag remelting (ESR) methods. Table 1. presents the initial conditions under which melting occurred in the VIM furnace.

The alloy's chemical composition was determined using optical emission spectrometry, utilizing a Spector 2004 model quantometer. The results, presented in Table 2. align with the AMS 5707J standards [11].

Table 1. VIM Furnace's Initial Melting Conditions.

Material of the mold	Dimensions of the mold (cm)	Total process time (min)	Holding time (min)	Melting amp (A)	melting voltage (V)	melting vacuum (mbar)	Primary vacuum (mbar)
Metal with zirconia coating	50×5 ×3	60-75	2-3	100-110	350-400	10	8×10^{-6}

Table 2. Waspaloy Alloy's Chemical Composition (Weight Percentage).

element	Ni	Cr	Co	Mo	Fe	Ti	Al	Si	Mn	Cu	C	Zr	P	B
AMS5707J	Bal	18-21	12-15	3.5-5	< 2	2.75-3.25	1.2-1.6	0.15<	<0.1	<0.1	0.02-0.1	0.02-0.08	<0.015	0.003-0.01
current study	Bal	19.1	13.4	4.2	0.95	3.9	1.6	0.08	0.01	0.011	0.05			

The ingot was homogenized at 1160 °C for four hours before undergoing hot rolling, as detailed in Table 3. The solution annealing procedure was conducted at 1050°C for a duration of four hours, followed by water quenching. Subsequently, a hot-worked strip with a thickness of 3 mm was cold rolled in four steps down to 1 mm. The hot and cold-worked specimens were then subjected to stabilization at 845°C for four hours. Finally, the specimens were aged at 730, 760 and 800 °C for durations of 1, 3, 9, 16 and 23 hours, followed by air cooling. It should be noted that the stabilization and aging cycle has been selected according to the TTT diagram of Waspaloy, as outlined in AMS 5544H and AMS 5707J standards [11, 12]. An ESE-Way5592 Vickers Hardness Testing Machine was employed to measure the hardness of the aged samples under a load of 30 kg. A hot tensile test was conducted at 538°C using an Instron 8502 model tensile machine, following the ASTM E8 standard [13].

The stress rupture test was carried out at 732 °C and 465 MPa in accordance with the ASTM E139 standard [14], using three replicate specimens per test, with the results averaged. The samples underwent standard [15] mechanical polishing and were etched using a waterless Kalling solution for between 3 to 7 minutes [13]. The microstructure was examined using Olympus Optical Microscope and a MIRA3 Tescan scanning electron microscope equipped with EDS analyzer set to 15 kV. The reported values for the size and volume fraction of γ' are the average values from four SEM micrographs on each sample. ASTM E112 test method was applied for determining the grain size. The γ' precipitates' volume fraction, precipitates size and grain size was measured using Image J Software.

3. Results and Discussion

3.1. Evaluation of Primary and Stabilized Microstructure

Fig. 1. presents the initial microstructure of the hot and cold-worked specimens. This microstructure features a (γ) matrix phase, and twins, as indicated by arrows in Fig. 1. Shear bands are also visible in the cold-worked specimen.

The formation of slip bands is attributed to two factors: the activation of various slip systems due to strain and the differential deformation of different parts of the grain in relation to the applied strain [16]. The formation of slip bands compensates for the difference between the deformation and the applied strain. These areas contain a significant amount of stored energy. The solutionized microstructure of the hot-rolled alloy is depicted in Fig. 2. This microstructure comprises γ phase, and twins as shown by arrows in Fig. 2. provides a detailed depiction of the hot-rolled specimen's microstructure, which notably includes the formation of several annealing twins.

Table 3. Waspaloy Alloy's Hot Rolling Conditions.

Primary Dimensions (mm)			Temperature (°C)	Final Dimensions (mm)			Cooling environment after rolling
length	width	thickness		length	width	thickness	
300	75	18	1160	1800	75	3	Water

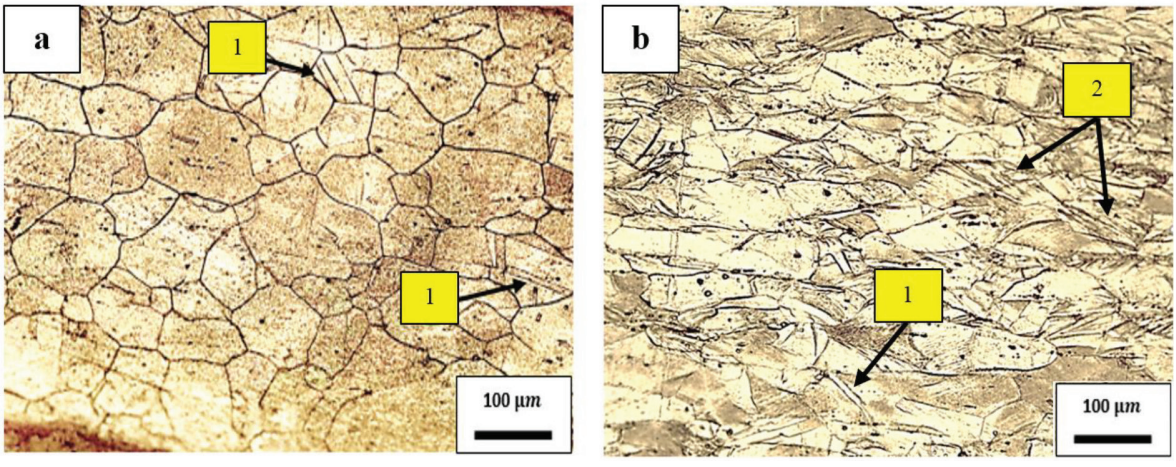

Fig. 1. Initial Microstructure of the Specimen Under a) Hot-worked and b) Cold-worked Conditions (1: Twins, 2: Slip Bands).

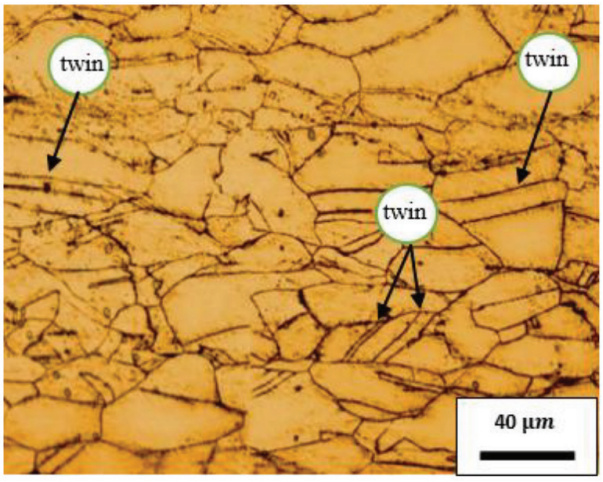

Fig. 2. Microstructure of Hot-worked Alloy Following Solution Treatment at 1050°C for 4 Hours.

Research has shown that alloys tend to release their energy at high energy points, resulting in a new arrangement at these locations due to the annealing effect, one component of which is the formation of twin arrangements. Annealing twins are a characteristic feature of materials with low stacking fault energy. Given that the alloy's matrix is austenitic, the presence of this type of twinning in the microstructure can be justified [16-18]. The non-uniform grain size distribution suggests that grain growth occurred during the annealing. The structure has fully recrystallized and begun to demonstrate slight grain growth. In Waspaloy, aging is typically conducted in multiple stages to achieve a dual precipitate size distribution. This spherical morphology of the γ' contributes to satisfactory strength across a broad temperature range. When two γ' size variants exist, dislocations can cut through finer precipitates and bypass the coarser ones. Consequently, with the added difficulty of dislocation movement, the strength significantly increases, and adequate ductility can be achieved. Alongside the impact of intermediate aging on the γ' characteristics, this process is utilized to reduce supersaturated carbon and form carbides at a lower energy level (Fig. 3). Supersaturated carbon at Waspaloy's intermediate heat treatment temperature results in the formation of spherical and discontinuous carbides at the grain boundaries, which can delay grain boundary sliding during creep at high temperatures. In a single-stage aging process, precipitates form within the matrix, whereas in a two-stage one, second-phase particles deposit both within the matrix and along the grain boundaries [19-20].

Fig. 4a and b. display the microstructure of the hot-worked and cold-worked specimens following stabilization at 845°C for 4 hours. The primary γ' precipitates' average size was measured as 150 nm for the hot-worked specimen and 170 nm for the cold-worked one. The γ' precipitates' volume fraction for hot-worked and cold-worked alloys was calculated to be 5 and 10 Vol%, respectively. In cold-worked samples, an increase in dislocation density, resulting from their multiplication, leads to a rise in stored energy.

As a result, the higher stored energy of the cold-worked samples releases to stimulate the formation of γ' precipitates [21]. Thus, in the cold-worked specimens, the volume fraction and size of the γ' phase are increased compared to the hot-worked ones.

3.2. Investigation of the Microstructure of Aged Waspaloy

Fig. 5. illustrates the optical microstructure of hot-worked and cold-worked specimens post-aging at temperatures of 730, 760 and 800 °C for 16 hours. The hot-worked specimen's microstructure comprises equiaxed grains, while the cold-worked specimen consists of austenite grains and twins oriented in the rolling direction. Fig. 6. illustrates the variation in grain size with respect to aging time and temperature for both hot- and cold-worked specimens. As the temperature increases, the average grain size of both the Cold and hot-worked alloy expands.

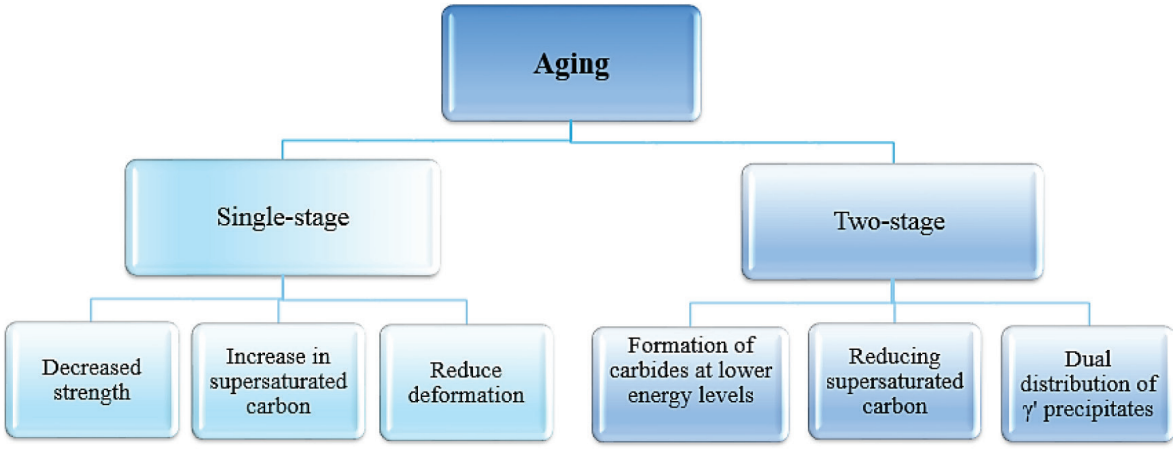

Fig. 3. Difference between single-stage and two-stage aging heat treatment.

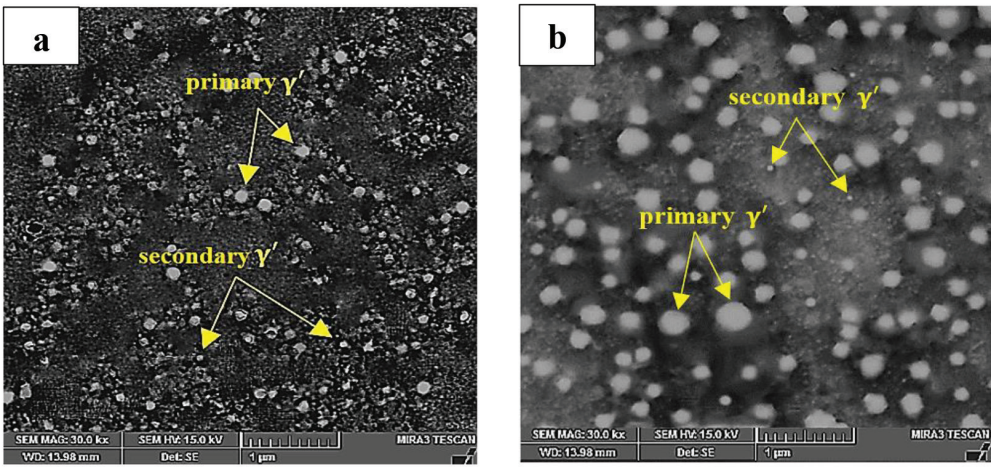

Fig. 4. Microstructure of a) Hot-worked and b) Cold-worked Alloys after Stabilization at 845°C for 4 hours.

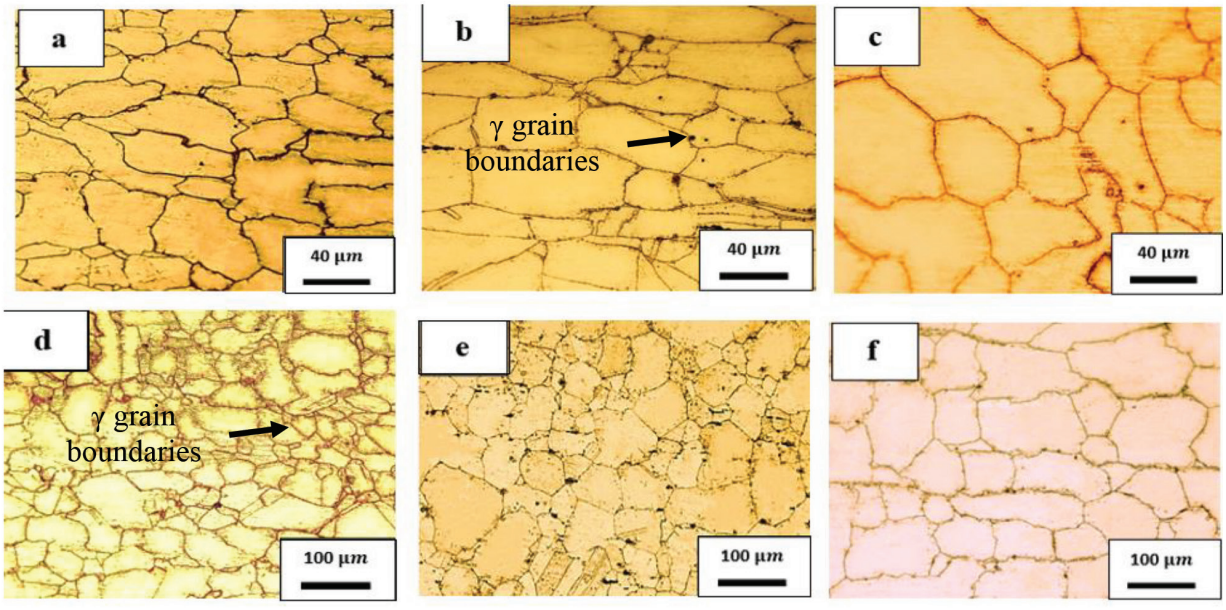

Fig. 5. Optical microscopic microstructure of hot-worked (a-b-c) and cold-worked (d-e-f) Waspaloy post aging at a, d) 730, b, e) 760 and c, f) 800°C for 16 hours.

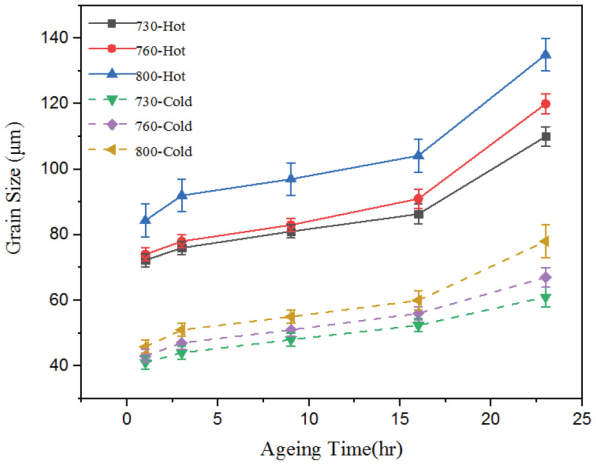

Fig. 6. Variation in grain size of hot and cold-worked specimens overaging time at temperatures of 730, 760 and 800 °C.

With the temperature climbing to 800 °C, the locking effect of the precipitates diminishes, promoting the migration of boundaries and leading to more substantial grain growth at elevated temperatures. The largest grain size in the hot-worked specimen is noted to be 139 µm after aging at 800°C for 23 hours. The reduced grain size of the cold-worked alloy, when compared to the hot-worked one, is caused by deformation [21]. Fig. 7. presents the FESEM microstructure of the hot-worked and cold-worked specimens after aging at 730, 760 and 800 °C for 16 hours.

A magnified image of γ' precipitates at 800°C is exhibited in Fig. 8. The alloys' microstructure encompasses γ phase, along with primary and secondary γ' precipitates. As depicted in Fig. 7. the average size and volume fraction of primary γ' precipitates at different temperatures were evaluated and analyzed for both hot- and cold-worked alloys, and are displayed in Fig. 9. Aging at higher temperatures increases the average size and volume fraction of primary γ' precipitates in both conditions.

The highest volume fraction of γ', reaching 34%, was obtained for the cold-worked alloy after aging at 800°C. It has been reported [21, 22] that cold working in nickel-based superalloys results in an increase in dislocation density with increasing deformation. Consequently, as the dislocation density increases, more preferred sites for γ' precipitate formation exist. This results in a greater formation of γ' precipitates and, thus, an elevated volume fraction of γ' precipitates in the cold-worked condition compared to the hot-worked one. Fig. 10. presents the FESEM microstructure and EDS analysis of the other phases following aging at 730 °C. It appears that, due to the high molybdenum content and based on its analysis, the phase indicated by A in Fig. 10a. could be M_6C. It forms when molybdenum or tungsten combines with

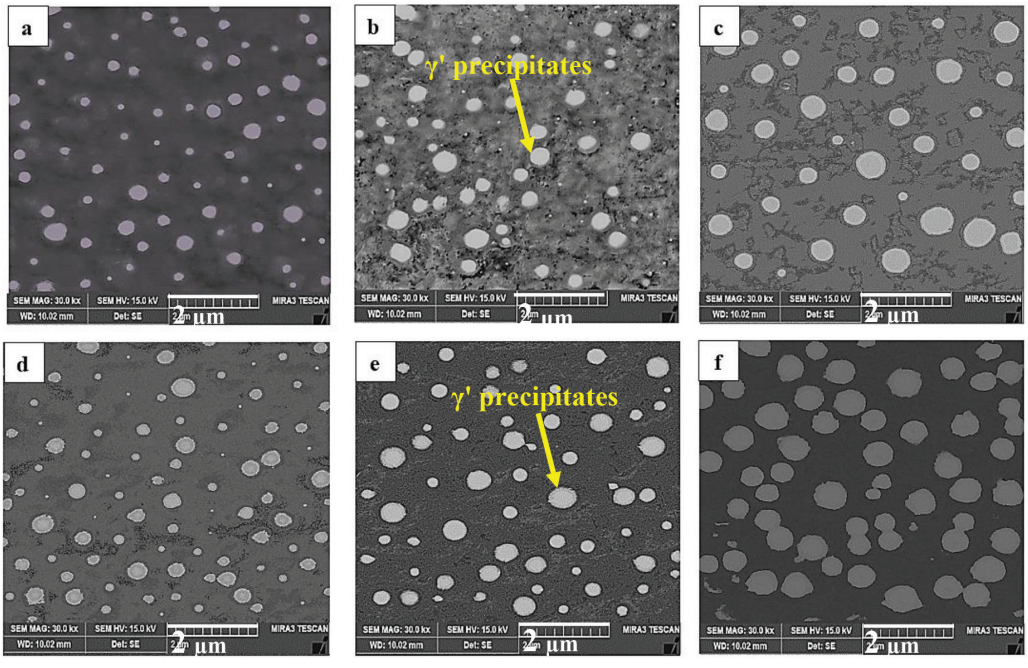

Fig. 7. FESEM micrographs of hot-worked (a-b-c) and cold-worked (d-e-f) specimens after aging at a, d) 730, b, e) 760 and c, f) 800°C for 16 hours.

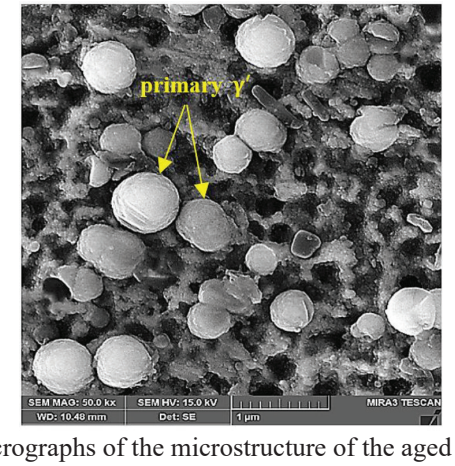

Fig. 8. FESEM micrographs of the microstructure of the aged specimen at 800 °C.

chromium to form alternative carbides. Given that M_6C carbides are more stable than $M_{23}C_6$ [3, 23], and they act as grain boundary pinning elements that control grain size during service, they hold substantial importance.

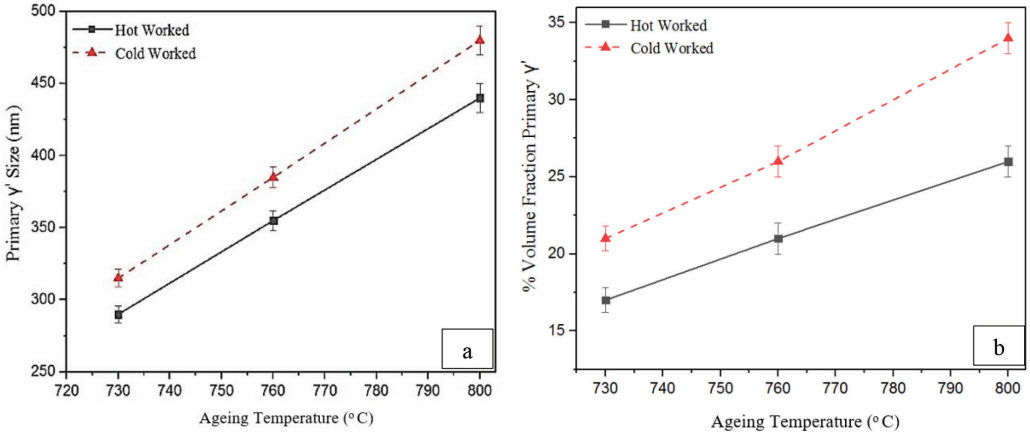

Fig. 9. Comparison of (a) the average size of primary γ' particles and (b) volume fraction of primary γ' phase for 16 hours after aging at temperatures of 730, 760 and 800 °C in the hot-worked and cold-worked specimens.

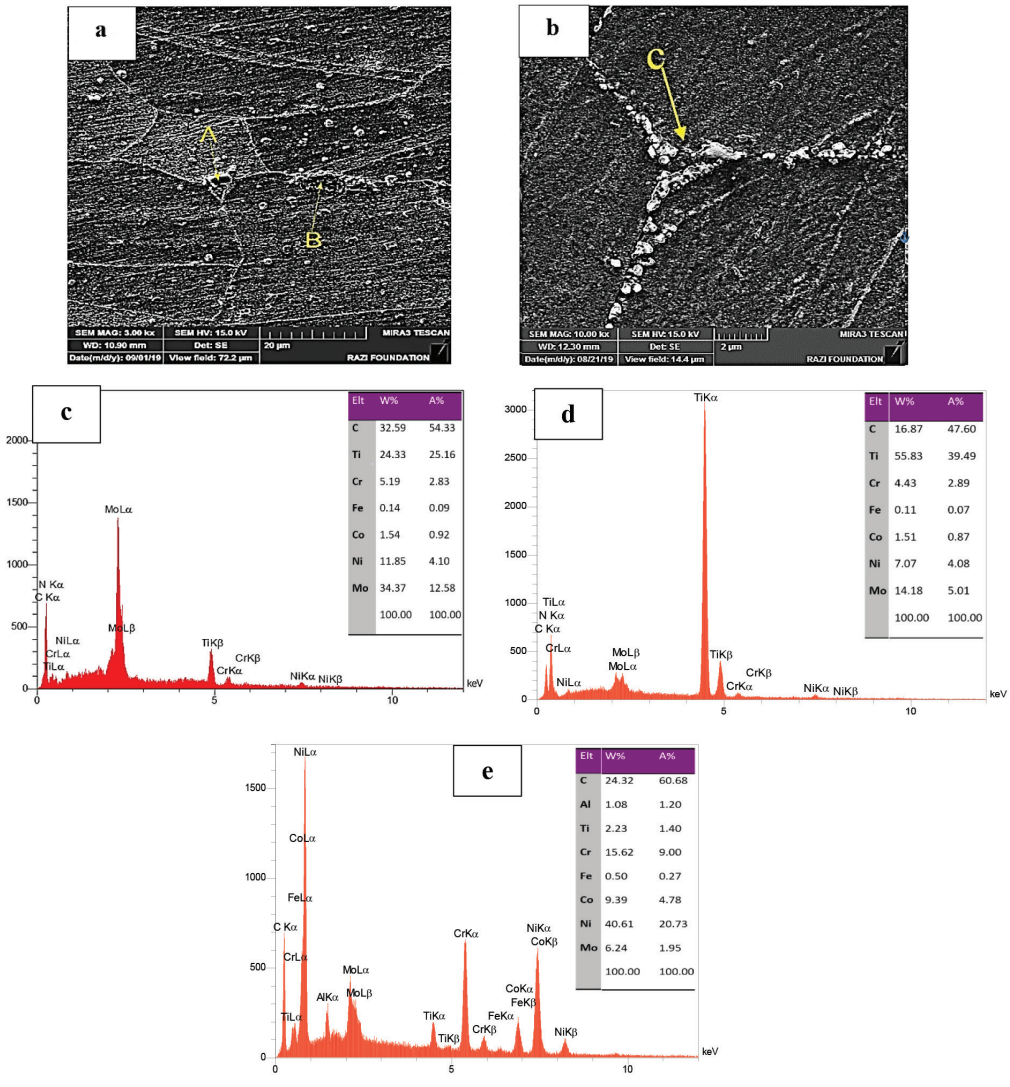

Fig. 10. (a, b) The FESEM microstructure of the cold-worked alloy post aging at 730°C. (molybdenum-rich (A), titanium-rich (B), and chromium-rich (C) grain boundary carbides) c) EDS analysis of molybdenum-rich carbide, d) titanium-rich carbide and e) chromium-rich carbide.

The principal aim of the aging process is the precipitation of the γ' phase and carbides and the achievement of an appropriate precipitate distribution within the Waspaloy structure. The secondary phase B in Fig 10a. which is rich in titanium, has a composition similar to that of TiC, formed during solidification. In Waspaloy, this carbide remains highly stable above 1038°C. This carbide is observed to have a random distribution within this alloy. The secondary phase, marked as C in Fig. 10b. is chromium-rich and closely resembles $M_{23}C_6$ in composition. The formation of this phase is of high importance. It is typically deposited in the form of cells and layers at the grain boundaries of nickel-based superalloys, preventing grain boundary sliding at high temperatures and thereby enhancing the alloy's strength at elevated temperatures [23].

3.3. Investigation of the Hardness of Aged Waspaloy

Fig. 11. compares the hardness of aged hot and cold-worked specimens at temperatures of 730, 760 and 800 °C. The highest Vickers hardness of 581 corresponds to the cold-worked alloy aged at 730°C, which possesses the smallest grain size of 42 μm, compared to the heat-treated alloy (grain size: 76 μm). As the hardness in the alloy increases and the grain size decreases, the strength and hardness of Waspaloy rise in accordance with the Hall-Patch relation [9, 24]:

$$\sigma_y = \sigma_0 + \frac{k_y}{\sqrt{d}} \qquad \text{Eq.(1)}$$

Where σ_y is the yield strength of the material, d is the grain size, and k_y is a constant that depends on the material. The grain boundaries serve as barriers to the movement of mobile dislocations. Their resistance to sliding thus increases in the alloy's strength and hardness [9, 24].

As shown in Fig. 12. for the hot-worked alloy at 730°C, the hardness begins to increase, albeit at a slower rate than in the cold-worked alloy, reaching its peak value of 550 Vickers after 9 hours of aging. As the temperature is increased to 760°C (after 9 hours) and 800°C (after 3 hours), the maximum hardness is achieved at these respective temperatures. The speed at which the maximum hardness is achieved increases with temperature. The hardness of the cold-worked alloy aged at 730°C begins to rise sharply, hitting its peak hardness of 581 Vickers after just 3 hours. By elevating the temperature to 760°C (after 3 hours) and then to 800°C (after only 1 hour), the hardness reaches its maximum value at these respective temperatures. As suggested by the chart, the hardness escalates more rapidly with increasing temperatures in the alloys, but the peak hardness value decreases as the temperature rises. Cold working, performed after solution treatment and before aging, affects phase stability. By carrying out cold working and controlling aging variables, the desired microstructure and mechanical properties, including hardness, can be achieved. Cold working enhances the density of dislocations, and studies [25, 26] suggest that this increased density elevates the work hardening rate. Dislocation density rises with cold work, providing nucleation sites for precipitates. It can be argued that at lower temperatures, dislocations drive the hardness to increase, but as the temperature rises, the effect of dislocations diminishes. In rolled specimens, the increase in hardness is due to an increase in dislocation density.

3.4. Investigation of the Hot Tensile Strength of Aged Waspaloy

The results of the hot tensile test of Waspaloy at 538 °C, in both cold and hot-worked conditions, aged at 730, 760 and 800 °C for 16 hours, are presented in Fig. 12. and Table 4. According to Table 4. the yield stress, ultimate tensile stress, and elongation of the hot- and cold-worked specimens in this research are higher than those stipulated by the AMS 5544 standard. A comparison of strength between hot and cold-worked specimens (refer to Fig .12.) reveals that the highest

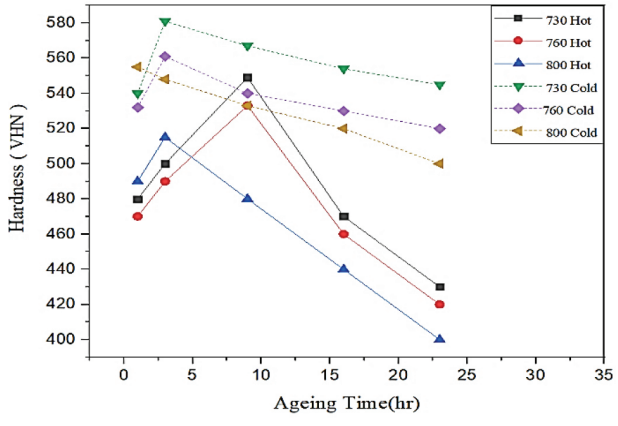

Fig. 11. Comparison of the hardness of hot-worked and cold-worked specimens aged at 730, 760 and 800 °C.

strength is attributed to the cold-worked specimens, characterized by the smallest grain size and a greater γ' volume fraction in comparison to their hot-worked counterparts. Since during cold working the production of dislocations increases, their interaction with each other increases their density. Therefore, the dislocations act as preferred sites for precipitate formation, which increases the density of precipitates. This, in turn, slows down and makes mobile dislocations more difficult due to the presence of precipitates. Thus, the alloy's strength increases. Therefore, the yield strength and ultimate tensile strength of the alloy in the cold-worked condition are higher than those in the hot-worked condition.

As depicted in Fig. 12. strength diminishes with an increase in the aging temperature for the specimens, attributable to the enlargement of grain size (see Fig. 6.) and γ' size (see Fig. 9a.). More slip systems are activated at elevated temperatures, and dislocation mobility heightens. This could be indicative of a shift in the dislocation movement mechanism, possibly due to coarsening of precipitation and an increased distance between precipitates. This leads to dislocations to bypass the precipitation via looping rather than cutting through them.

This signifies a shift in the threshold where strength starts to decline and the mechanism of dislocations passing through precipitates undergoes a change. As precipitation becomes coarser, its locking effect lessens, promoting grain boundary migration and easier grain growth [27, 29]. One key mechanism for failure in nickel-based superalloys is the initiation and growth of voids through grain boundary sliding [30]. The superior tensile strength of these specimens can be attributed to the further decomposition of $M_{23}C_6$ carbides at 730°C and their discrete precipitation along grain boundaries, which contributes to the strengthening of superalloy grain boundaries [31]. Fig. 13. depicts the variation curves of elongation with aging temperature. The ductility of specimens increases with temperature, achieving a maximum ductility of 36% and 19.55% for hot-worked and cold-worked specimens, respectively, at 800°C.

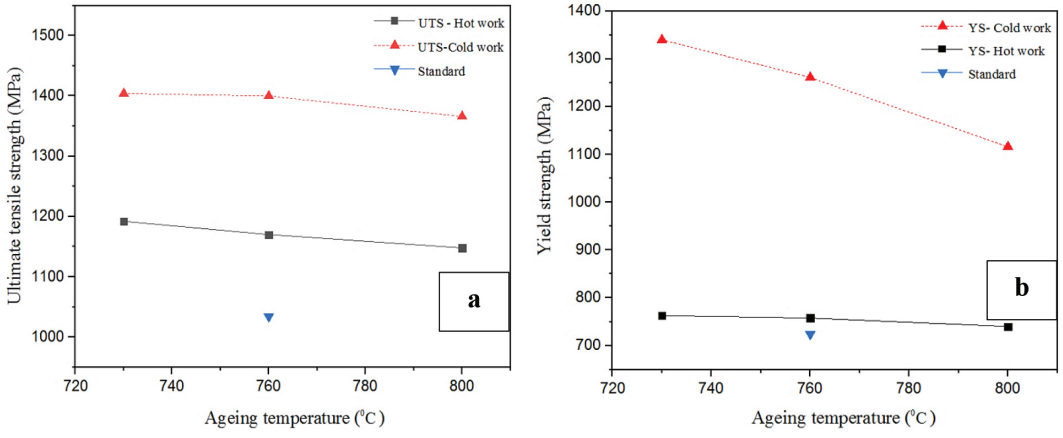

Fig. 12. Variation of (a) ultimate tensile strength and (b) yield strength by aging temperature for the hot-worked and cold-worked specimens.

Table 4. Results of high temperature mechanical properties test under aging for the hot-worked and cold-worked specimens.

Temperature (°C)	Sample name and conditions	Elongation %	Yield Strength (MPa)	Tensile Strength (MPa)	Stress Rupture (hr)
Standard[11,12]	standard	15	724	1034	23
730	cold-worked	16.32	1340	1404	46
	hot-worked	28.26	763	1192	36
760	cold-worked	18.30	1261	1400	-
	hot-worked	35	758	1170	-
800	cold-worked	19.55	1116	1366	-
	hot-worked	36	740	1148	-

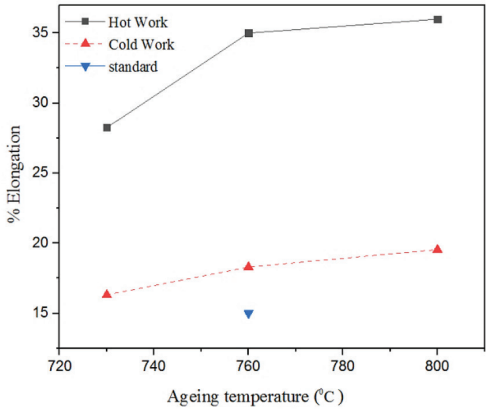

Fig. 13. The alteration in elongation with aging temperature for hot-worked and cold-worked specimens.

As the temperature increases, dislocation mobility and the uniformity of dislocation distribution also increase, facilitating deformation and leading to a decrease in yield strength. Comparing elongation variations between hot-worked and cold-worked specimens as per Fig. 13. the most significant alterations in elongation pertain to hot-worked specimens. Studies suggest that with an increasing work hardening rate and diminishing grain size due to increased dislocation density (dislocation forest) and a decrease in slip systems, the strength rises while ductility recedes in cold-worked specimens. With the increase in aging temperature, dislocation climb occurs, and the Orowan mechanism becomes dominant [32]. At high temperatures, with a growing size of γ' particles and increased distance between them, dislocations are uniformly dispersed within the matrix and rarely move by cutting precipitates. The bending of dislocations and formation of dislocation rings around γ' particles can be additional observations at high temperatures [33]. An increase in temperature facilitates dislocation movement, subsequently leading to an enhanced percentage of elongation and a decrease in strength. It is also evident that slip via grain boundaries occurs much more quickly at high temperatures than dislocation slip within the grains. Thus, grain boundaries partially serve as a source of weakness at elevated temperatures, and the deformation rate of the alloy intensifies under such conditions [33, 34].

In summary, the ductility of Waspaloy is a critical factor in its overall performance, especially in demanding service conditions. By optimizing its microstructure and processing, Waspaloy can achieve the necessary balance of strength and ductility for reliable and efficient operation in aerospace applications. This has been added to the text.

3.5. Investigation of the Stress Rupture of Aged Waspaloy

Exploring the Stress Rupture Properties of Aged Waspaloy. Fig. 14. depicts the curve representing the correlation between rupture life and strain for the alloy in both hot- and cold-worked states, post-aging at 730 °C.

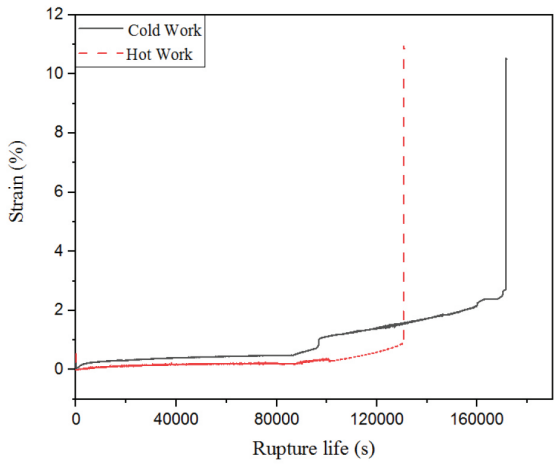

Fig. 14. The curve representing rupture life vs. strain for the hot-worked and cold-worked specimens aged at 730 °C for 16 hr.

Stress rupture test outcomes indicate that the lifetime of stress rupture is 46 hours for the cold-worked alloy and 36 hours for the hot-worked specimen. According to AMS 5544, this should be 23 hours. Thereby, the results of this research exceed the standards. The rupture life of the specimen appears to be significantly influenced by the volume fraction of γ' precipitates and grain boundary carbides, specifically of the M_6C and $M_{23}C_6$ types. As demonstrated in Fig. 8a. the cold-worked specimen, endowed with a higher volume fraction of γ' precipitates, outperforms the hot-worked sample by displaying a more extended rupture life. In this study, the extended rupture life is attributed to the formation of γ' precipitates, consistent with the Nabarro–Herring theory [4, 35]. The stress rupture curve illustrates that the initial creep stage, which indicates a decrease in creep rate, is brief for each specimen due to the high temperature and test stress. As is evident, the first stage of creep is characterized by the dominance of the work-hardening mechanism resulting from the interaction of subgrains over the softening caused by creep. An almost constant creep rate characterizes the second creep stage. The steady-state creep rate of the second stage of creep results from the balance between the mechanisms of work hardening and recovery. The consistent strain rate of the second stage symbolizes a stable microstructure. Table 5. presents the minimum creep rate (slope of the graph in the second stage) for different specimens. It can be observed that the minimum creep rate of the cold-worked alloy is lower than that of the hot-worked specimen, implying a stable microstructure at high temperatures. The creep in the third stage and the eventual rupture of the sample are accompanied by the initiation and growth of microcracks, which is attributed to the existing porosity. According to Fig. 13. the cold-worked specimen spends minimal time in the third stage. The onset of the third stage is marked by the formation of cracks and internal voids in rupture metals [4, 35].

Table 5. Minimum creep rate of hot worked and cold worked alloys (aged at 730 ℃ for 16 hours).

Alloy	Hot work	Cold work
Minimum creep rate (mm/sec)	1.9×10^{-6}	1.24×10^{-6}

The second stage for the cold-worked specimen significantly outlasts that of the hot-worked alloy, leading to the inference that with an increase in work hardening, and as a result of enlarging γ' size and volume fraction, the cold-worked alloy exhibits desirable properties.

Creep behavior can be rationalized by considering factors like the size of γ' precipitates, the volume fraction of γ' precipitates, and the number of carbides. When the alloy is subjected to high-temperature conditions, the size and appropriate volume fraction of γ' precipitates can play a pivotal role in ensuring optimal performance. However, it appears that the positioning and size of the carbides also significantly contribute to this mechanism. Typically, an increase in the γ' volume fraction and the number of carbides correlates with a longer creep life. This is because γ' and carbides serve as barriers to dislocation movement, thereby strengthening the superalloy. γ' and carbides can resist grain boundary sliding and migration during the creep process. Furthermore, a longer rupture time can be attributed to a lower creep rate in a steady state stage [4, 5, 23].

4. Conclusions

This research aimed to explore the effect of heat treatment on the microstructure and high-temperature mechanical properties of the Waspaloy alloy. The findings are as follows:

- The average primary γ' size and volume fraction exhibit an upward trend during aging at temperatures of 730, 760 and 800°C for both hot and cold-worked specimens. The cold-worked specimen showed the highest values, with an average primary γ' size of 480 nm and a volume fraction of 33%.
- The highest high-temperature tensile properties are associated with the cold-worked specimens aged at 730 °C for 16 hours, boasting a yield strength of 1340 MPa and an ultimate strength of 1404 MPa. It is worth noting that this temperature yielded the smallest grain size, the largest size of initial γ' precipitates, and the highest γ' volume fraction for the cold-worked sample.
- An increase in the aging temperature from 730 to 800 °C leads to a rise in the ductility of both hot and cold-worked specimens, with the maximum ductility at 800 ℃ being 36% and 19% for hot and cold-worked specimens, respectively.
- The rupture life of the cold and hot-worked alloy amounts to 46 and 36 hours, respectively, a phenomenon attributable to the higher volume fraction of γ' in the cold-worked specimen. This results in a 27.78% improvement in the properties of the alloy in the cold-worked condition compared to the hot-worked one.

Acknowledgments:

The source of financial grants and other funds was supported by Malek Ashtar University of Technology.

References

[1] Kulawinski D, Henkel S, Holländer D, Thiele M,Gampe U, Biermann H, Fatigue behavior of the nickel-base superalloy Waspaloy™ under proportional biaxial-planar loading at high temperature, Int J Fatigue. 2014; 67: 212-9.

[2] Liu G, Kong L, Xiao X, Birosca S, Microstructure evolution and phase transformation in a nickel-based superalloy with varying Ti/Al ratios: Part 1-Microstructure evolution, Mater Sci Eng A. 2022; 831: 142228.

[3] Chen X, Yao Z, Dong J, Shen H, Wang Y, The effect of stress on primary MC carbides degeneration of Waspaloy during long term thermal exposure, J Alloys Compd. 2018; 735: 928-37.

[4] Wang H, Liu D, Wang J, Yang Y, Wang L, Wang H, et al. Role of size and amount of γ' phase on creep properties of Waspaloy, Mater Charact. 2021; 181: 111498.

[5] Chang K.M, Liu X, Effect of γ′ content on the mechanical behavior of the Waspaloy alloy system, Mater Sci Eng A. 2001; 308: 1-8.

[6] Polkowska A, Lech S, Polkowski W, The effect of cold rolling degree on microstructure, crystallographic texture and mechanical properties of Haynes® 282® wrought nickel superalloy, Mater Sci Eng A. 2020; 787: 139478.

[7] Dieter G.E, Mechanical Metallurgy. 3rd ed. New York: McGraw-Hill Book Co.; 1986.

[8] John V.B, Testing of Materials. 2nd ed. London: Macmillan Education LTD; 1992.

[9] Stefan O, Wretland A, Sjöberg G, The effect of grain size and hardness of Waspaloy on the wear of cemented carbide tools, Int J Adv Manuf Technol. 2010; 50: 907-15.

[10] Whelchel R.L, Kelekanjeri V.G, Gerhardt R.A, Ilavsky J, Effect of aging treatment on the microstructure and resistivity of a nickel-base superalloy, Metall Mater Trans A. 2011; 42: 1362-72.

[11] AMS 5544. Aerospace Material Specification. AMS International; 2000.

[12] AMS 5707J. Aerospace Material Specification. ASTM International; 2000. ASTM E8. Standard test

method for tension testing of metallic materials. West Conshohocken: ASTM International; 2004.
[13] ASTM E139. Standard Test Methods for Conducting Creep, Creep-Rupture, and Stress-Rupture Tests of Metallic Materials. ASTM International; 2011.
[14] Geddes B. Superalloys: Alloying and Performance. 1st ed. USA: ASM International; 2010.
[15] Humphreys F.J, Hatherly M, Recrystallization and related annealing phenomena. 1st ed. London: Elsevier; 2012.
[16] Jiang H, Xiang X, Dong J, The morphology and characteristics evolution of MC carbide during homogenization in hard-to-deform superalloy GH4975, J Alloys Compd. 2022; 929: 167086.
[17] Liu H, Zhao X, Dong J, Zheng L, Inhomogeneous planar distribution of γ′ precipitates in Waspaloy caused by local spatial consumption of MC carbides, J Mater Eng Perform. 2022; 31: 1397-404.
[18] Seetharaman V, Rao K.B.S, Mannan S.L, Rodriguez P, Microstructure and mechanical properties of a Nimonic PE 16 superalloy subjected to double-aging treatments, Mater Sci Eng A. 1984; 63(1): 35-50.
[19] Caliari F.R, Candioto K.C, Couto A.A, Nunes C.Â, Reis D.A, Effect of double aging heat treatment on the short-term creep behavior of the Inconel 718, J Mater Eng Perform. 2016; 25: 2307-17.
[20] Liu H, Zhang M, Xu M, Meng Y, Xu G, Ta N, et al. Microstructure evolution dependence of work-hardening characteristic in cold deformation of a difficult-to-deform nickel-based superalloy, Mater Sci Eng A. 2021; 800: 140280.
[21] Ran R, Wang Y, Zhang Y.X, Fang F, Wang H.S, Yuan G, et al. Microstructure, precipitates and mechanical properties of Inconel 718 alloy produced by two-stage cold rolling method, Mater Sci Eng A. 2020; 793: 139860.
[22] Song X, Wang Y, Zhao X, Zhang J, Li Y, Wang Y, et al. Analysis of carbide transformation in MC-M23C6 and its effect on mechanical properties of Ni-based superalloy, J Alloys Compd. 2022; 911: 164959.
[23] Liu G, Kong L, Xiao X, Birosca S, Microstructure evolution and phase transformation in a nickel-based superalloy with varying Ti/Al ratios: Part 2–Phase transformation, Mater Sci Eng A. 2022; 831: 142229.
[24] Zhang S.H, Ye N.Y, Cheng M, Song H.W, Zhou H, Wang P.B, Effect of cold rolling and heat treatment on the mechanical properties of GH4169 alloy sheet at room temperature, Metals. 2015; 6(1): 1-11.
[25] Liu J, Zhang W, Mei F, Xin X, Cao Y, Zhu C, et al. Microstructure evolution and work hardening behaviour during cold deformation of Haynes 214 superalloy, J Mater Res Technol. 2023; 24: 5792-804.
[26] Zhang X.Y, Li H.P, Bai J.M, Li X.K, Jia J, Liu C.S, et al. The evolution of γ′ precipitates and hardness response of a novel PM Ni-based superalloy during thermal exposure, J Alloys Compd. 2023; 168757.
[27] Yamaguchi Y, Tajima R, Terada Y, Evolution of γ′ precipitates for wrought Ni-based superalloys, Mater Trans. 2020; 61(11): 2185-94.
[28] Bessa S.M, de Oliveira C.A, Effects of a high temperature artificial aging on microstructure and mechanical properties of the Ni-base superalloy GTD-111, Mater Charact. 2023; 201: 112966.
[29] Sujata M, Madan M, Raghavendra K, Venkataswamy M.A, Bhaumik S.K, Identification of failure mechanisms in nickel base superalloy turbine blades through microstructural study, Eng Fail Anal. 2010; 17(6): 1436-46.
[30] Lee T.H, Suh H.Y, Lee J.H. Precipitation behavior of $M_{23}C_6$ carbides and its effect on mechanical properties of Ni-based Alloy 690, J Nucl Sci Technol. 2021; 58(1): 45-50.
[31] Peng T, Wang Y, Yang B, Yang G, Tensile properties and deformation mechanisms of Nimonic 105 superalloy at different temperatures, Mater Sci Eng A. 2021; 828: 142028.
[32] Cui L, Su H, Yu J, Liu J, Jin T, Sun X, Temperature dependence of tensile properties and deformation behaviors of nickel-base superalloy M951G, Mater Sci Eng A. 2017; 696: 323-30.
[33] Zhang P, Yuan Y, Yin H, Gu Y, Wang J, Yang M, et al. Tensile properties and deformation mechanisms of Haynes 282 at various temperatures, Metall Mater Trans A. 2018; 49: 1571-8.
[34] Brassart L, Delannay F, Bounds for shear viscosity in Nabarro–Herring–Coble creep, Mech Mater. 2019; 137: 103106.
[35] Brassart L, Delannay F, Bounds for shear viscosity in Nabarro–Herring–Coble creep, Mech. 2019; 137: 103106.